Endourethral MRI

[1]H.H. Quick, [1]H.K. Pannu, [2]R. Genadry, [1,3]E. Atalar

Departments of [1]Radiology, [2]Obstetrics and Gynecology, and [3]Biomedical Engineering
Johns Hopkins University, Baltimore, Maryland, USA
Dr. E. Atalar is a founder and consultant of Surgi-Vision Inc.

Introduction

Detailed anatomic information about the female urethra and pelvic floor is currently not available by any diagnostic imaging technique. This information would provide a significant contribution to the understanding of urinary incontinence and other urethral abnormalities and would contribute to the surgical approach for treatment and therefore patient management (1,2).

This study introduces an endourethral approach for ultra-high resolution MR imaging of the female urethra and the periurethral tissues. To this end, two different radiofrequency (RF) receiver coil designs for an endourethral insertion have been developed: a single-loop coil and a quadrature/phased array coil (3). The performance of the coils has been evaluated in human female cadaver pelvic studies. The novel endourethral approach provided a dramatic increase in signal-to-noise ratio (SNR) at the region of interest.

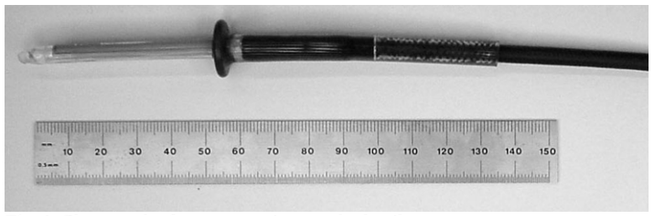

Fig. 1: Photograph of a prototype intraurethral coil.

Methods

Prototype endourethral single-loop as well as quadrature RF receiver coils were designed (Fig. 1). Both designs feature a flexible coil circuit, tuning/matching directly at the coil, active decoupling, and the integration of a λ/4 coaxial choke to decrease unbalanced currents and limit potential RF heating effects (Fig. 2) (4). Effective reduction of the mutual inductance between the two coils of the quadrature design was achieved by introducing a metallic "paddle" (4) to steer the flux between the coils. The active region of the coils was 50 mm in length. The whole assembly was housed in a biocompatible polymeric tubing with an outer diameter of 15 F (5 mm). During clinical use, the distal end (5-6 cm) of the coil will be inserted in the urethra, while the coil electronics as well as the mouth of the cable choke will remain outside of the body. A stopper ring prevents the coil from being inserted further into the urethra.

The coils' imaging performance was evaluated in one formalin fixated as well as in six freshly harvested female human cadaver pelvises. The coils were introduced into the urethra with the tip entering the bladder approximately 5 mm. This position ensured that the whole urethra was covered by the highest signal intensity and homogeneity of the coil. Imaging was performed on a 1.5T Signa LX-2 EchoSpeed (GE Medical Systems, Milwaukee, WI). High-resolution fast spin-echo (FSE) T2-weighted imaging of the whole urethra was acquired axial to the urethra coil. Imaging parameters were: FSE 8 echoes; TR/TE 2000/78 ms; FOV 30x30 mm; matrix 320x192; 6 NEX; BW 15.6 kHz; slice 1.5 mm; imaging time, 4:48 min. For ultra high-resolution imaging, the in-plane resolution was increased by reducing the FOV to 20x20 mm and using a 256x256 matrix. Imaging time was 8:32 min with 8 NEX.

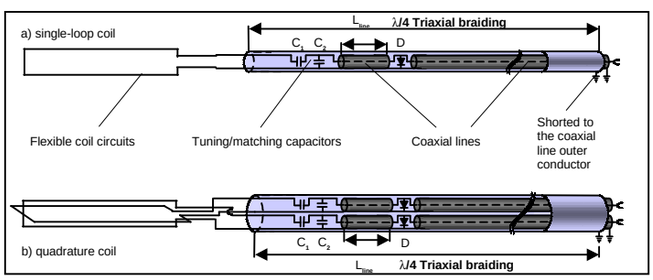

Fig. 2: Schematic of the intraurethral coils: a) single-loop coil, and b) quadrature coil, showing the impedance matching capacitors, *C*, a PIN diode, *D*, for active decoupling of the receiver coils, and the λ/4 braiding forming a coaxial choke.

An image intensity correction (IIC) algorithm was applied to compensate for the B_1 signal variation of the coils across the small FOVs. The applied post processing method allowed the coil position and angle to be entered interactively.

Histologic correlation of the MR images was achieved by removing the urethra *en bloc* from the unfixed cadavers. The specimen were fixed by suspension in 10% buffered formalin. They were then embedded in paraffin and 6 μm thick axial sections were cut and stained with Trichrome staining on glass slides.

Results

The quality factor, *Q*, of the loaded coils was determined to be 67 for the single-loop and 80 and 74 for the quadrature coils, respectively. The impedance of the coaxial chokes was Z = 750 Ω. The paddle enabled an isolation of both coils of 50 dB without loss of performance.

Small FOV (30x30 mm) axial imaging with the endourethral coils enabled the visualization of all layers of the urethra in high-resolution. Signal penetration depth beyond the urethra was sufficient to depict the pubic bone anterior to, and the vagina posterior to the urethra. Post-processing and display of the images with the IIC reliably removed B_1 inhomogeneities, and thus facilitated the visualization of structures adjacent to the coil. Image contrast increased, resulting in better depict-ability of the different urethra wall layers (Fig. 3). Further decrease of the FOV to 20x20 mm increased the in-plane resolution to 78x78 μm, which enabled the resolution even of single folds of the urethral mucosa (Fig. 4).

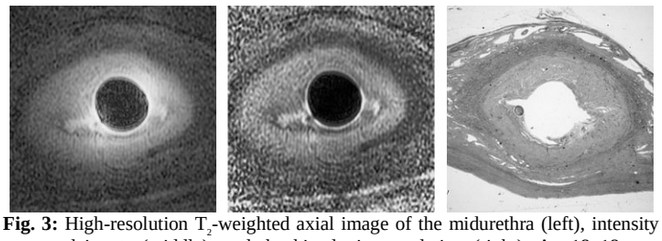

Fig. 3: High-resolution T_2-weighted axial image of the midurethra (left), intensity corrected image (middle), and the histologic correlation (right). An 18x18 mm image portion is shown. In-plane resolution was 94x156 μm, slice thickness, 1.5 mm. Note the increased image contrast following intensity correction.

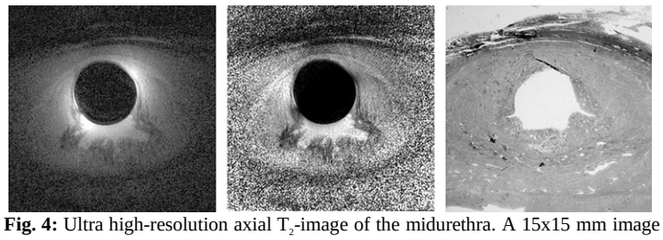

Fig. 4: Ultra high-resolution axial T_2-image of the midurethra. A 15x15 mm image portion is shown. In-plane resolution was 78x78 μm, slice thickness, 1.5 mm. Single folds of the mucosa can be depicted.

Conclusion

The prototype MR receiver coils for the novel endourethral approach described in this report have been designed for clinical use in human subjects and are currently undergoing testing to determine their efficiency in the evaluation of female urethral pathology. The experimental data of this study has proven that endourethral MRI can provide very high-resolution images of the female urethra and surrounding tissues. The higher achievable local SNR and therefore higher spatial resolution compared to a pelvic array, transrectal, or even endovaginal approach for coil placement adds valuable information to the controversial discussions about female urethral anatomy.

References

1 Siegelman, E.S., et al., Radiographics 17:349-365, 1997.
2 Tan, I.L., et al., Radiology 206(3):777-783, 1998.
3 Atalar, E., et al., Proc. of 4th ISMRM, 1731, 1996.
4 Ladd, M.E., Quick, H.H., Proc. of 7th ISMRM, 104, 1999.
5 Hoult, D.I., et al., MRM 1:339-353, 1984.